Investigation of TiAlN, AlTiN, and TiAlSiN Coated Inserts on the Machining Performance of AISI 420 Steel and Multi-Objective Optimization of Process Parameters

Moganapriya Chinnasamy[1] · Rajasekar Rathanasamy[2] · Sathish Kumar Palaniappan[1] · Samir Kumar Pal[1]

Abstract The impact of cutting parameters on the SR of machined work piece and tool flank wear during machining of AISI 420 martensitic stainless steel is studied in the research study. PVD-CAE coated TiAlN, AlTiN, and TiAlSiN cutting tool inserts were employed for machining. The potential influence of cutting parameters was determined using analysis of variance. To optimise the process parameters influencing roughness and tool wear, Taguchi methodology based L9 orthogonal array was selected. A multi-objective optimization strategy based on grey relation and fuzzy control had been employed in this investigation. Grey relation analysis was used to improve the process parameters, which were then fuzzified using the Mamdani fuzzy engine. The parameter combination of speed 120 m/min, CD − 1.5 mm, F − 0.1 mm/rev and TiAlN coating was proven to be the best optimized setting.

Keywords Martensitic stainless steel · TiAlN · AlTiN · TiAlSiN · Taguchi

Introduction

Martensitic stainless steels have a high strength-to-weight ratio and are used in high-strength applications such as medical instruments, shaving blades, and bearings. 420 grade martensitic stainless steel parades high resistance to corrosion as similar to type 410 but it is stronger and harder. In both the annealed and hardened states, it is magnetic. Only completely cured or fully hardened and stress relieved steels provide maximum corrosion resistance. It is hardly used in the annealed state. The microstructural composition and thickness of carburized layer produced on AISI 420 MSS may be adjusted by appropriately regulating the carburizing temperature. Micro-structural analysis reveals that minimum temperature and limited duration of heat treatment enhance the resistivity of carburized materials [1]. Because of the process, characteristics and microstructure, martensitic stainless steels deteriorate ploughing or abrasive wear. To increase the wear and corrosion resistance of martensitic stainless steels, surface treatment techniques and coatings are recommended. The most likely surface treatment method appears to be plasma nitride, which is an outstanding solution for improving the wear resistance of dry contacting surfaces [2]. Both industrial and theoretical techniques, assessment of tool life have a more scientific approach [3]. The surface integrity investigation of AISI 420 for various machining variables and machining condition states that the machining variables such as velocity of cutting, feed (F), nose radius and the tool are considered for microhardness of the machined outcome. It also discloses that the rate of tool feed is the most important output responses [4]. Carbide tools coated using TiAlN alternating layers outperformed uncoated tools in terms of tool flank wear and mean roughness [5]. Chips have a considerable impact on the machining process, especially the surface quality. With all F, a greater number of chips were created at low cutting (CS) [6]. In face turning, the consequences of WR have a direct influence on the surface quality of the machined product, whereas flank wear decreases somewhat with increasing feed and CS and cutting depth (CD) [7].

✉ Rajasekar Rathanasamy
  rajasekar.cr@gmail.com

1 Department of Mining Engineering, Indian Institute of Technology Kharagpur, Kharagpur, West Bengal, India

2 Department of Mechanical Engineering, Kongu Engineering College, Erode, Tamilnadu, India

564

J. Inst. Eng. India Ser. D (July–December 2022) 103(2):563–573

With a larger nose radius, the surface quality was noticeably improved. The results revealed that the CS is the most influential parameter on surface roughness (SR) [8]. The AM samples built at angular powder deposition against the horizontal base improved the mechanical properties and minimized the directionality challenges [9]. The results indicate that the tools costs are insignificant and considers cost effective with ecological machining condition [10].

The optimum machining setting for multi objective statistical ANOVA confirmed that F has the strongest influence on the SR [11–15]. The revolutionary changes in machine were appropriate choice of tool attribution to the development or invention of cemented carbide tools possessing superior properties [16, 17]. A researcher presented a new parameter-free ANFIS construction approach called KERNEL. It is capable of doing optimum architecture estimation as well as optimal SSD in a timely and effective manner. It can fine-tune the current knowledge base and in the absence of domain experience, it can uncover the ideal knowledge. A novel quick and flexible SSD approach based on hypercube sampling (HC) is given to allow optimal size determination [18].

In enterprises and academics, performing multi-objective optimization under uncertainty is a regular necessity. For scattered and discontinuous data in uncertain domain, it is difficult to get reliable data through robust optimization. An author presented a data-driven technique in which a unique fuzzy clustering process was employed alongside boundary creation to transcribe the uncertain space in order to identify particular locations of uncertainty. Following that, samples are created in the mapped uncertain zones using smart Sobol sampling [19]. A multi-objective optimization formulation under uncertainty has been presented, which can lead to simultaneous maximisation of productivity and reduction in energy consumption. Among the different strategies for dealing with uncertainty, Chance Constrained Programming (CCP) is thought to be the most efficient. DDCCP (Data-Driven CCP) is a revolutionary technique that combines machine learning algorithms with CCP, making the approach data-driven. A unique fuzzy clustering approach is applied to structure uncertain space in such a way that particular regions of uncertainty are precisely detected depending on the uncertain data for more realistic sampling, ultimately influencing the best solution accuracy [20].

The specimen cooled with chilled air has a higher resistance to corrosion behaviour after a longer period of time [21]. The tools with CVD coating presented a better performance than the PVD for the cutting conditions used [22, 23]. Undissolved carbides and tempering carbides were discovered in the martensitic matrix by using optical microscopy, scanning electron microscopy (SEM), and atomic force microscopy (AFM). When the spindle speed is increased, the SR decreases, which is important during turning operation [24]. Texturing is thought to alter tribological activity in the sliding region, as the results showed that the texture model that starts from a distance of 1 m performed better [25]. Untreated coated tools display obvious delamination of the coating, which has been successfully limited by using microblasting [26].

The use of the desirability function (DF) for multi objective performance parameter optimization reveals that there is no single best solution [11, 27]. The optimal combination of cutting speed, feed, cutting depth, and cooling mechanism for decreasing SR and maximising material removal rate (MRR) while maximizing tool life was determined using Taguchi-based entropy weighted grey relational analysis [28]. The machining characteristics (SR, cutting force) are determined by changing the range of cutting parameters [29]. Cold nitrogen gas and oil mist conditions boost machining responses as compared to dry machining. Avoiding emulsion cooling, lower waste costs, and longer tool life minimize unit production costs as compared to wet machining [30]. Abrasion and diffusion were the dominant wear mechanisms in martensitic stainless steel machining, while attrition and abrasion were dominant in super martensitic stainless steel machining [31]. TiAlN-coated tool steel has a far higher hardness than the uncoated tool steel [32]. As wear rate (WR) increases, the roughness characteristics change. The mean and total roughness metrics are essential for determining tool life based on surface quality [33, 34]. This paper mainly focuses on investigating the effect of TiAlN, AlTiN, and TiAlSiN coated inserts on the performance of AISI 420 steel by varying CD, F and CS. This paper also identifies the optimised process parameter which majorly influences SR and WR.

Materials and Methods

In this experimental study, uncoated CNC inserts obtained from Usman Tools, Coimbatore were utilized. The insert is finished into 40 mm diamond bar with length of 1.2 cm and nose radius 0.8 mm. The inserts with negative rake angle are aligned to the specification of CNMG-120408. Hard coatings such as titanium aluminium nitride (TiAlN), aluminium titanium nitride (AlTiN) and titanium aluminium silicon nitride (TiAlSiN) were deposited on cutting tool through PVD technique in Famex Coating Private Limited at Coimbatore. The photographical images of coated inserts are depicted in Fig. 1a–c.

The microhardness of all inserts were determined by using (Model: Wilson400 series) by applying 1 kg load for
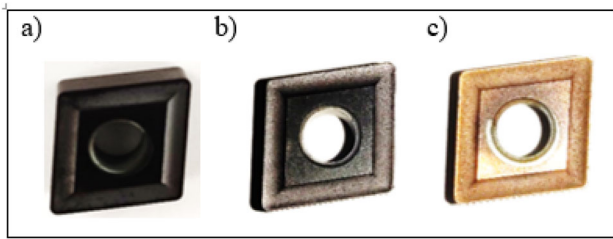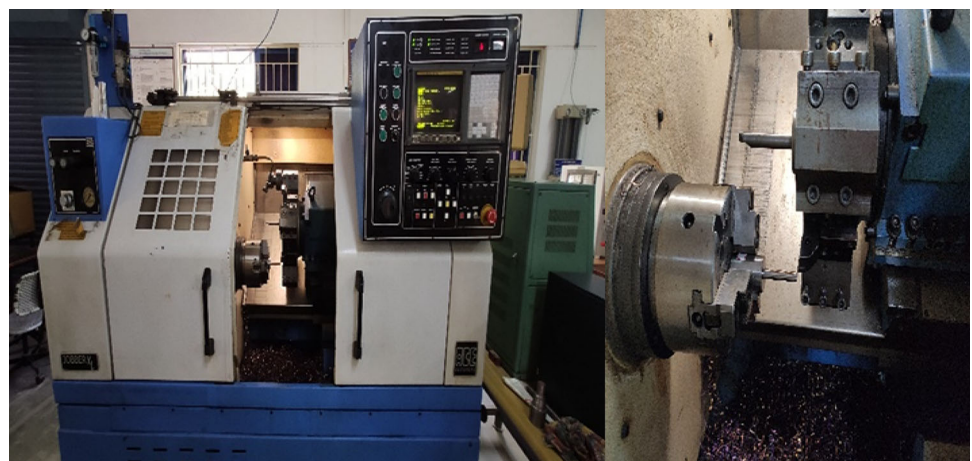
Fig. 1 **a** TiAlN **b** AlTiN **c** TiAlSiN

10 s. For these tests, a diamond indenter was used. The tests were conducted in accordance with ASTM E- 384–17. The hardness was reported as an average of three measurements to minimize the irregularity effects of coating. The hardness of the work piece (AISI 420 martensitic stainless steel) was determined using the Rockwell Hardness Tester. The test was carried out in C-scale with a diamond indenter and a 150 kg load.

AISI 420 martensitic stainless steels were utilized for this research study. The steel rod was 36 mm in diameter. The long rod was cut into 9 pieces of length 100 mm using cutting machine and its ends were faced using manual lathe. The JOBBER XL numerical controlled turning centre was employed for the research experiments as shown in Fig. 2. Table 1 indicates the different parameters and their levels, which are used to carry out the experiments.

With various combinations of input parameters, Taguchi optimization was employed to produce better order of machining sequence. This research experimentation used a L9 orthogonal array as shown in Table 2. All nine experiments were carried out with the different input setting. SR, MRR and WR were calculated as output responses during machining using an orthogonal array. For each trial, three trails were completed, and the average value was recorded.

SR was found through surface tester with 1-inch travel length in X-axis with the 0.5 mm/s as average run speed. The mass variation of coated CNC tool inserts before and after machining was used to calculate WR. The mass variation of work piece before and after turning was used to determine MRR. Coating, CS, F and CD were the variables in this experiment. SR (Ra and Rz), WR and MRR were all optimized using an optimization approach that included GRA and fuzzy logic approach. Grey analysis and fuzzy logic values were matched, and the best optimized result was discovered.

Since the Taguchi design strategy is meant to optimize just one solution characteristics, the GRA optimizes a variety of outcomes. GRA was chosen based on literature survey to optimize multiple responses: SR (Ra and Rz), MRR and WR. The optimization process in GRA is divided into three phases.

When the experimental data have minimum-the-better characteristic, the measured data can be normalised by using Eq. (1).

$$\mathrm{Xi(p)} = \frac{\max \mathrm{xi(p)} - \mathrm{xi(p)}}{\max \mathrm{xi(p)} - \min \mathrm{xi(p)}} \qquad (1)$$

where $\mathrm{X_i(p)}$ = normalized value. $\mathrm{x_i(p)}$ = experimental output value. $\max \mathrm{x_i(p)}$ = maximum of $\mathrm{p^{th}}$ response. $\min \mathrm{x_i(p)}$ = minimum of $\mathrm{p^{th}}$ response.

When the experimental data have higher-the-better characteristic, the measured data can be normalised by using Eq. (2).

$$\mathrm{Xi(p)} = \frac{\mathrm{yi(p)} - \min \mathrm{yi(p)}}{\max \mathrm{yi(p)} - \min \mathrm{y(p)}} \qquad (2)$$

Then, the grey relational coefficient can be calculated by using Eq. (3)

Fig. 2 Turning of AISI 420 Stainless steel

566

J. Inst. Eng. India Ser. D (July–December 2022) 103(2):563–573

Table 1 Machining parameters

Parameter	Condition
CS in m/min	120, 160, 200
F in mm/rev	0.10, 0.15, 0.20
CD in mm	0.5, 1.0, 1.5
Tool	TiAlN, AlTiN, TiAlSiN
Work piece	AISI 420 martensitic stainless steel (36 mm diameter, 100 mm length)
Coolant	No coolant, dry cutting environment

Table 2 L9 orthogonal array

Exp no	Coating	CS (m/min)	F (mm/rev)	CD (mm)
1	TiAlN	120	0.10	0.5
2	TiAlN	160	0.15	1.0
3	TiAlN	200	0.20	1.5
4	AlTiN	120	0.15	1.5
5	AlTiN	160	0.20	0.5
6	AlTiN	200	0.10	1.0
7	TiAlSiN	120	0.20	1.0
8	TiAlSiN	160	0.10	1.5
9	TiAlSiN	200	0.15	0.5

Table 3 Hardness values of different coated tools in HV

Sl. no	TiAlN	AlTiN	TiAlSiN
1	1779	2302	1820
2	1716	1646	1796
3	1763	1799	1855
Avg	1753	1916	1824

$$\xi i(p) = \frac{\Delta \min + \Psi \Delta \max}{\Delta 0i(p) + \Psi \Delta \max} \qquad (3)$$

where $\xi_{i(p)}$ = grey relation coefficient. $\Delta_{0i}(p) = \|X_0(p)-X_i(p)\| \Psi$ = distinguishing coefficient (0.5). $\Delta \min$ = minimum of Δ_{0i}. $\Delta \max$ = maximum of Δ_{0i}.

Databases are used to extract membership functions, which are then used to generate fuzzy rules. The decision-making unit is used to infer from the developed laws. Based on the degree of matching, the fuzzification interface translates the input into linguistic words. The fuzzy effects

are then converted into crisp production by the defuzzification tool. Then, the obtained grades were fuzzified using fuzzy approach.

Results and Discussion

TiAlN, AlTiN, TiAlSiN coating applied on the tungsten carbide CNC insert had increased hardness as depicted in Table 3. The hardness of TiAlN, AlTiN, TiAlSiN coated inserts was determined and better hardness (1916 HV) was apparent for AlTiN as compared to TiAlN and TiAlSiN coated inserts. WR, SR, and MRR are the machining data that were obtained from experimentation as listed in Table 4.

The machined samples are shown in Fig. 3. Analysis of variance has been performed for all the output responses individually, and the data were depicted in Tables 5, 6, 7 and 8.

GRA has been selected in order to optimize numerous responses. The output responses were normalized according to a method based on the GRA technique and the absolute values were recorded. The grey ratio coefficients for the responses from the normalized values were calculated, and the values were described in Table 9. Weights were allocated as 0.5 for each grey coefficient. The grey relationship coefficients of the individual response were computed from GRG average. The results were ranked based on final GRG and the experiment number 1 (CS: 120 m/min, F: 0.1 mm/rev, CD: 0.5 mm and TiAlN coating) was ranked with highest grade.

The inputs to fuzzy logic system included CS, feed, CD, and coating. Input parameters can be described for instance in linguistic membership, which is low, medium and high. The average grey grades of separate outputs have also been determined as the input for fuzzy logic interface and the attainment of relational grey grade is represented by very small, very medium small, very small, very large, very medium high and very high attributes. Table 10 shows the interval of sorting. Depending on the technique, a combination of 9 fuzzy guidelines was allocated. By adjusting the fuzzy logic, maximum – minimum combination action provides results as shown in Fig. 4. Finally, the defuzzifier changes predicted outputs to GFRG, as illustrated in Fig. 5, by utilizing MATLAB (R2016b) fuzzy logic toolbox. Table 6 summarizes the outcomes of the GFRG.

As described in Table 10 and Fig. 6, settings for experiment number 1 were optimized: 120 m/min CS, 0.1 mm/rev F, 0.5 mm CD, coating: TiAlN). For all GRG and associated GFRG trials, the relative assessment is shown in Fig. 6. From Fig. 6, the highest values of GRA

Table 4 Machining data

Tool coating	CS m/min	F mm/rev	CD mm	SR Ra, μm	SR Rz, μm	MRRkg/s	WR m³/sec
TiAlN	120	0.10	0.5	0.185	1.062	3.79 E-06	3.57E-12
TiAlN	160	0.15	1.0	0.617	3.230	1.09 E-05	6.98 E-12
TiAlN	200	0.20	1.5	0.455	2.483	2.19 E-05	5.43 E-12
AlTiN	120	0.15	1.5	0.341	1.687	1.10 E-05	2.15 E-11
AlTiN	160	0.20	0.5	0.622	2.933	1.71 E-05	3.97 E-11
AlTiN	200	0.10	1.0	0.648	2.901	9.30 E-06	5.39 E-12
TiAlSiN	120	0.20	1.0	0.567	2.611	2.49 E-05	9.27 E-12
TiAlSiN	160	0.10	1.5	0.377	2.040	8.70 E-06	2.13 E-11
TiAlSiN	200	0.15	0.5	0.497	2.361	2.19 E-05	2.5 E-11

Fig. 3 Machined work pieces

Table 5 Analysis of variance for Ra

Source	DF	Adj SS	Adj MS	F-Value	p-Value
Coating	2	0.05435	0.027175	16.53	0.002
CS	2	0.01971	0.009855	5.83	0.025
F	2	0.02382	0.011910	7.17	0.014
CD	2	0.32779	0.163895	49.78	0.001
Total	8	0.43146			

Table 6 Analysis of variance for Rz

Source	DF	Adj SS	Adj MS	F-Value	p-Value
Coating	2	0.09686	0.04843	11.54	0.008
CS	2	1.55340	0.77670	7.92	0.032
F	2	0.69813	0.34907	5.39	0.046
CD	2	1.34726	0.67363	2.48	0.082
Total	8	3.69566			

Table 7 Analysis of Variance for WR

Source	DF	Adj SS	Adj MS	F-Value	p-value
Coating	2	0.00034	0.00017	1.28	0.045
CS	2	0.00056	0.00028	1.99	0.034
F	2	0.00030	0.00015	1.18	0.044
CD	2	0.00013	0.00002	2.87	0.063
Total	8	0.00133			

Table 8 Analysis of variance for MRR

Source	DF	Adj SS	Adj MS	F-Value	p-value
Coating	2	0.27432	0.137108	34.21	0.028
CS	2	0.18440	0.092700	23.13	0.041
F	2	1.06843	0.533715	133.15	0.007
CD	2	0.00812	0.004008	1.89	0.053
Total	8	1.53507			

Table 9 Grey analysis results

Sl. no	Ra, grey coefficient εi (k)	Rz, grey coefficient εi (k)	MRR, grey coefficient εi (k)	WR, grey coefficient εi (k)	Grey relational grade ε (xo, xi)	Grey rank
1	1.000	1.000	0.333	1.000	0.833	1
2	0.349	0.333	0.413	0.841	0.484	7
3	0.462	0.433	1.000	0.907	0.700	2
4	0.597	0.634	0.490	0.501	0.556	3
5	0.346	0.367	0.503	0.333	0.387	9
6	0.333	0.371	0.412	0.909	0.506	6
7	0.378	0.412	0.470	0.760	0.505	5
8	0.547	0.526	0.437	0.505	0.504	4
9	0.426	0.455	0.477	0.457	0.454	8

Table 10 Fuzzy analysis results

| CS	F	CD	Coating	Grey analysis output	Fuzzy logic analysis grade
Low	Low	Low	Low	Very very high	0.946
Medium	Medium	Medium	Low	Small	0.499
High	High	High	Low	Small	0.725
Low	Medium	High	Medium	Small	0.571
Medium	High	Low	Medium	Very very small	0.410
High	Low	Medium	Medium	Small	0.529
Low	High	Medium	High	Very small	0.523
Medium	Low	High	High	Small	0.519
High	Medium	Low	High	Very small	0.469
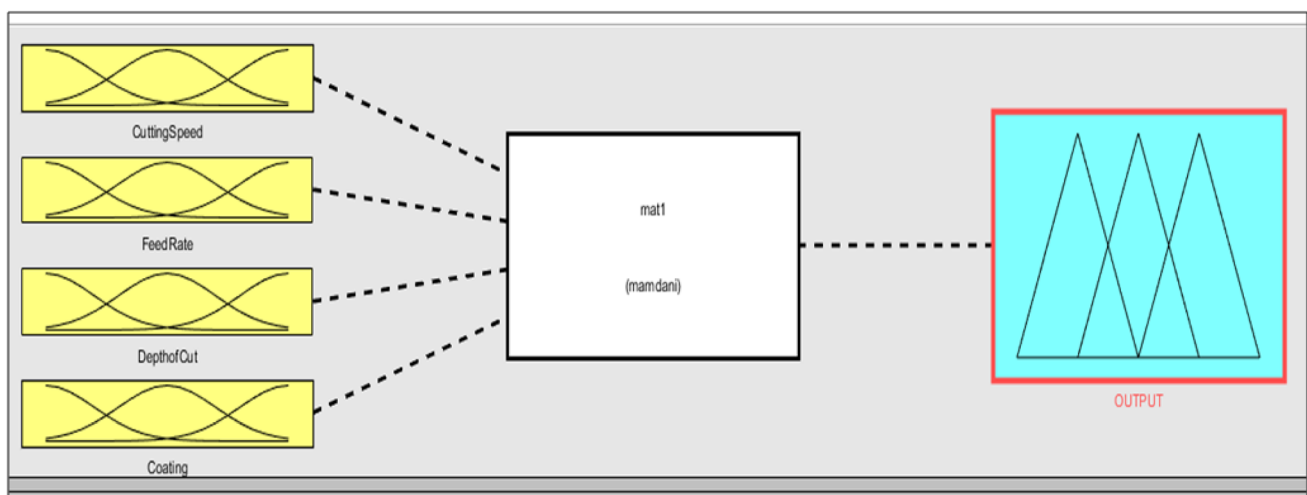
Fig. 4 Fuzzy logic designer
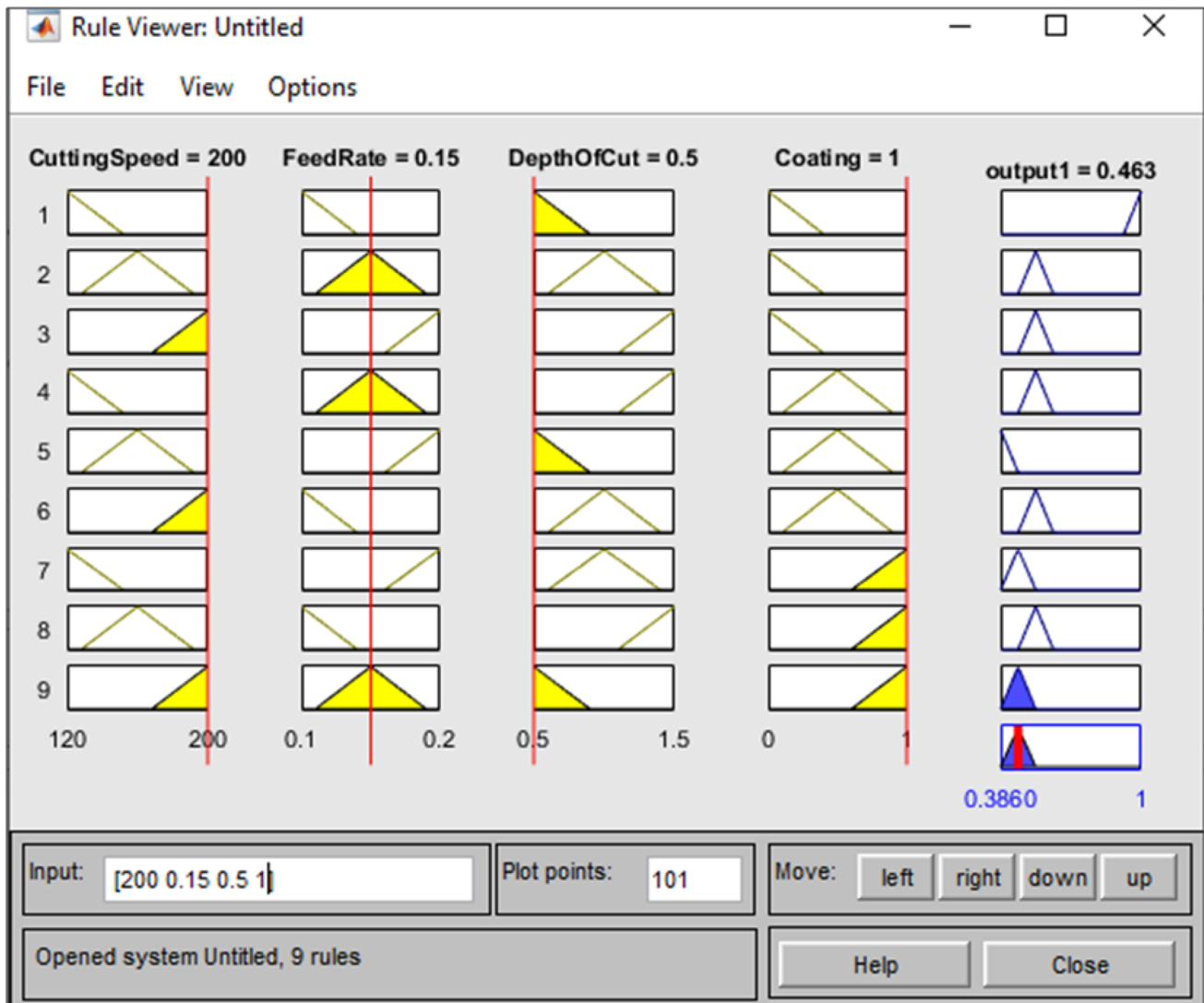
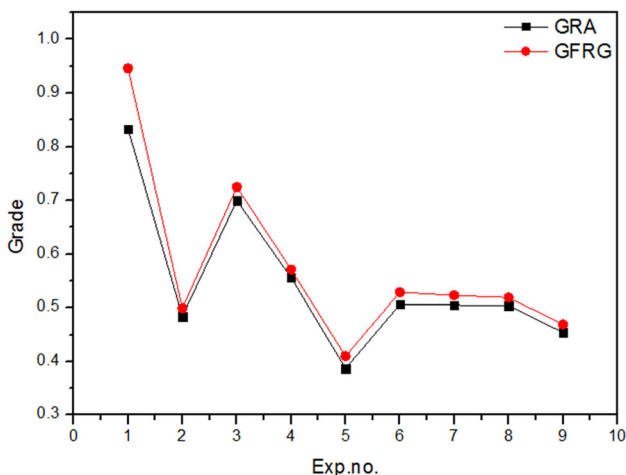Fig. 5 Fuzzy logic designer rule viewer

Fig. 6 Comparison of GRA and GFRG

and GFRG were observed for experiment 1 based on L9 orthogonal array. Hence, the experiment 1 was the final optimized setting. The GFRG has higher grade than GRA. It was improved by 2.4% compared with GRA.

After obtaining GFRG, the Taguchi method was used for optimizing the results of GFRG. GFRG was considered as output for 9 experiments. The optimized setting was found to be Coating: TiAlN, CS: 120 m/min, F: 0.10 mm/rev and CD: 1.5 mm for achieving higher GFRG as depicted in Fig. 7. To validate the results of this optimization technique, an experiment was performed with an
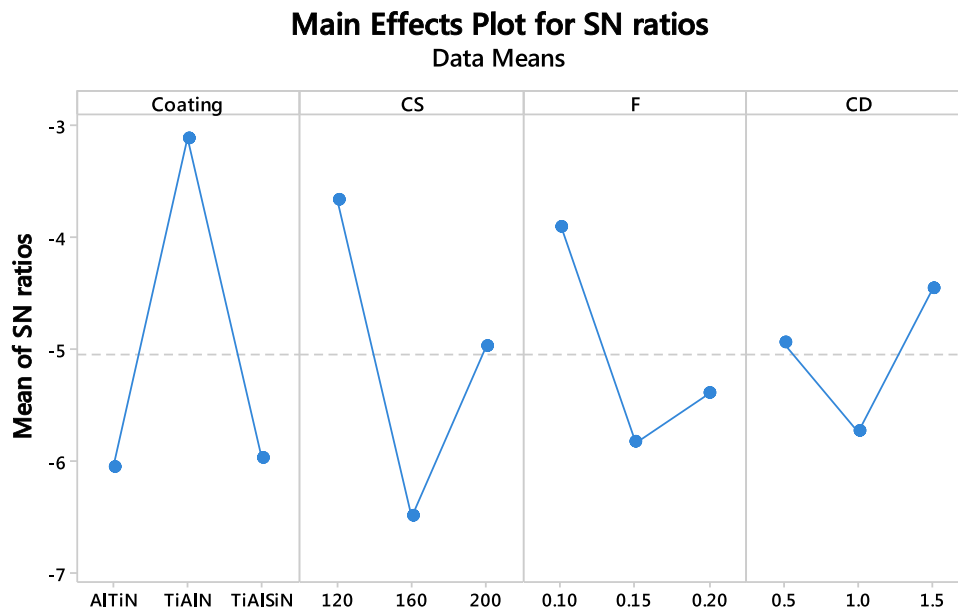
Fig. 7 Optimized setting for GFRG

Main Effects Plot for SN ratios
Data Means

Table 11 Confirmation experiment

Responses	Optimal parameters		
	Predicted value from GFRG A1B1C1D1	Optimized experimental value A2B1C1D3	Difference in values
Ra	0.185	0.172	0.013
Rz	1.062	1.023	0.039
MRR	3.79 E-6	1.10 E-5	0.000721
WR	3.57 E-12	9.87 E-12	6.3 E-12

optimized combination (A2B1C1D3) and the outputs were measured and presented as shown in Table 11.

After machining, the tool inserts were examined through microscope with magnification 100 X. The WR was observed as shown in below Fig. 8 a–i.

During machining, the chip formations were observed. The chip formation of various experiments is shown in below Fig. 9 a–i. In general, Golden colour chips denotes less WR, whereas blue burnt denotes more WR. The creation of the chip, which has a substantial effect on tool life, has been largely affected by CS, CD and F. It can be ascribed to changes in the material inertia among shear planes during machining. By increasing CS, the cutting force rises, and therefore the bending moment of the chip increases. This chip might damage the tool further by generating heat. The chip thickness has decreased for each feed with decreasing CS. Though, the average chip thickness similarly dropped with reduction of F. Hence, as the CS, the F considerably impacts chip thickness.
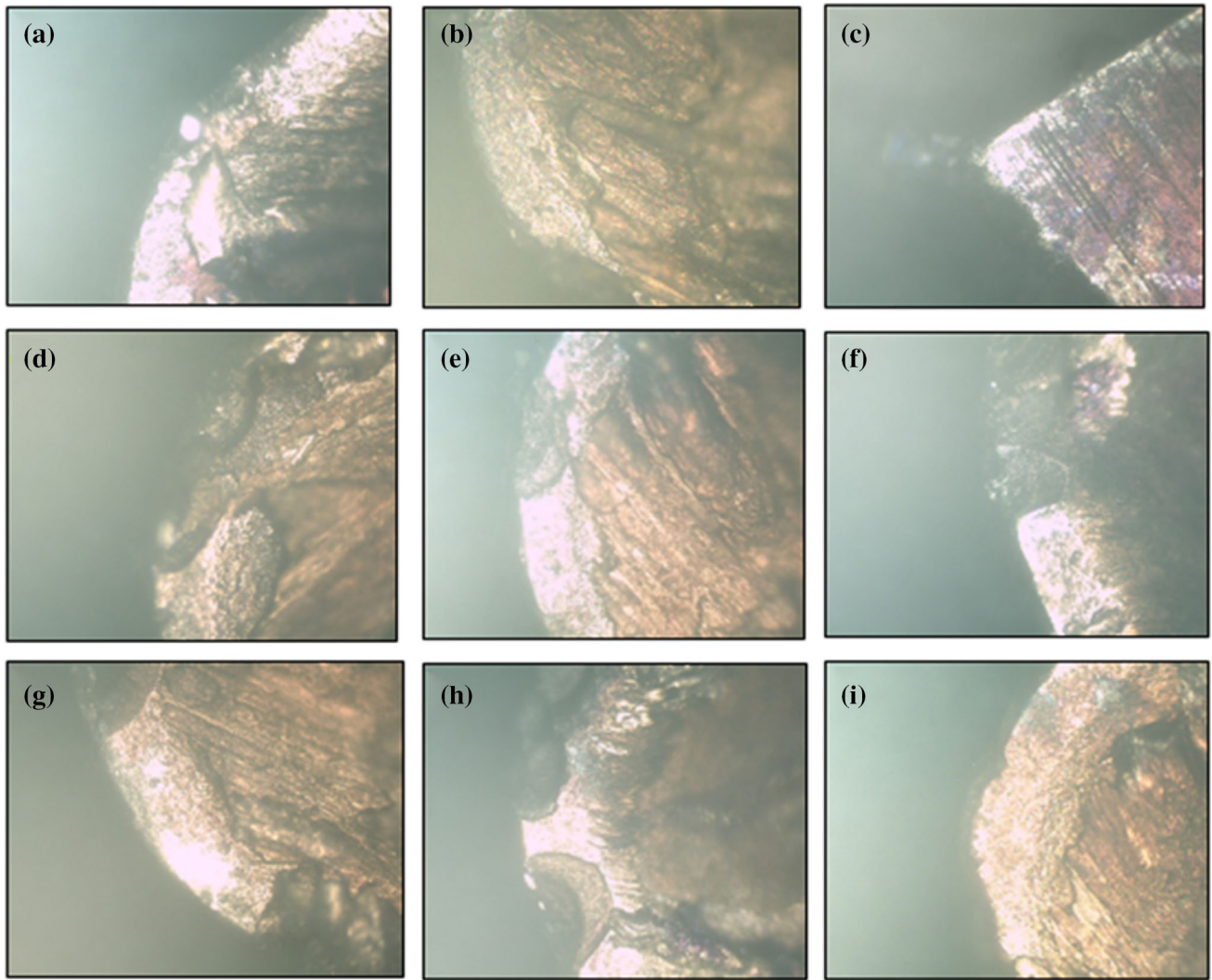
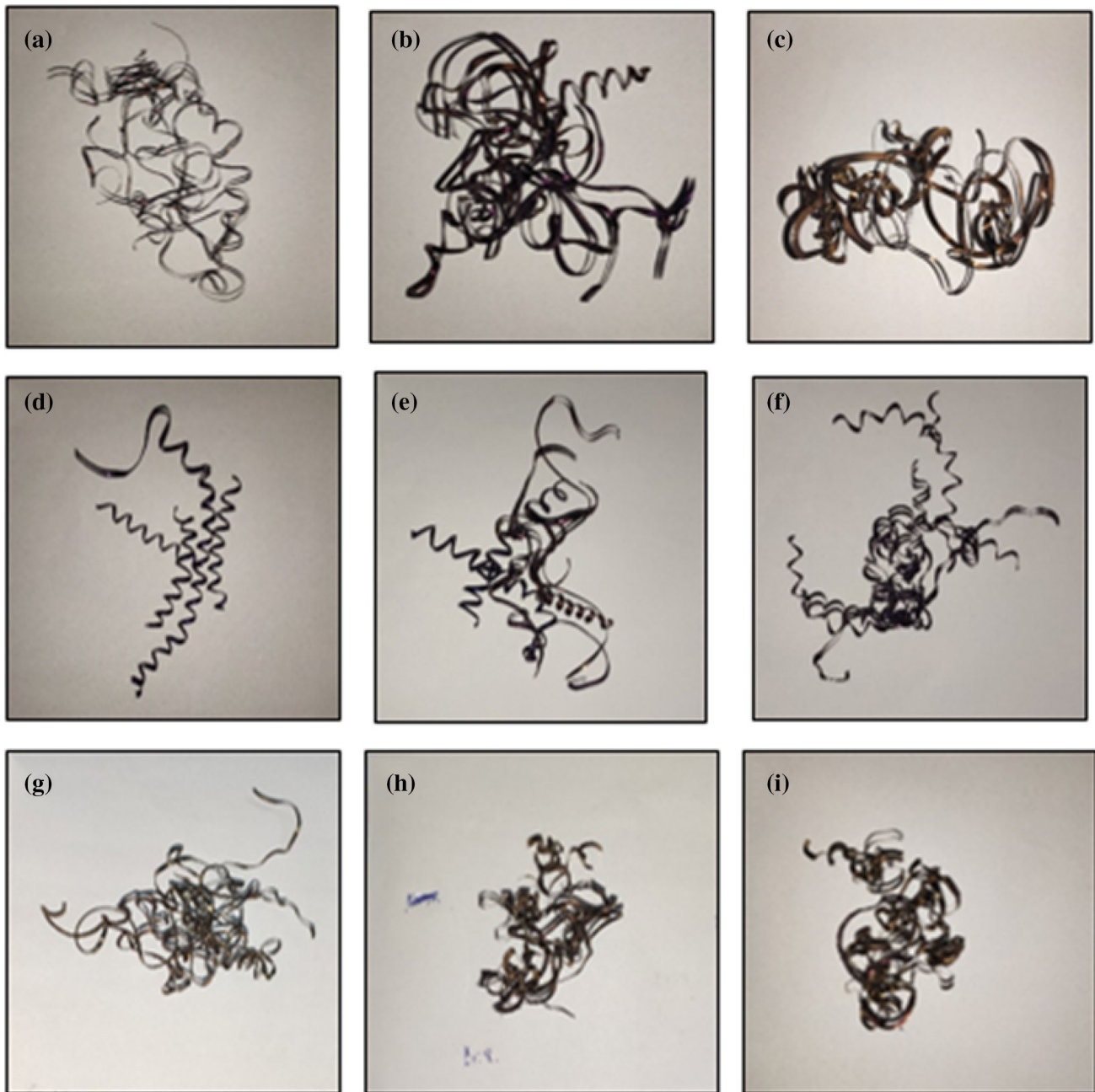**Fig. 8** a–i Microscopic images of tool for experiments 1–9

572

J. Inst. Eng. India Ser. D (July–December 2022) 103(2):563–573

Fig. 9 a–i Images of cutting chips for experiments 1–9

Conclusions

TiAlN, AlTiN, TiAlSiN coated inserts were effectively deposited on the outer surface of cutting tools. Experimentation was planned based on L9 orthogonal array. CS, F, CD and coating material were taken as the operating parameters. All the machining tests were performed based on run order and the output responses such as Ra, Rz, WR and MRR were measured. These output responses have been optimized simultaneously through grey fuzzy optimization technique. Initially, the several responses were normalized and converted into single grade through GRA. Later, these grades were fuzzied using fuzzy logic tool box. From the results of GRA and GFRG, experiment number 1 was found to be the optimized setting (120 m/min CS, 0.1 mm/rev F, 0.5 mm CD, and coating: TiAlN). GFRG is then optimized through Taguchi experiment and it was found that Coating: TiAlN, CS: 120 m/min, F: 0.10 mm/rev and CD: 1.5 mm were the optimized setting for turning AISI 420 martensitic stainless steel.

J. Inst. Eng. India Ser. D (July–December 2022) 103(2):563–573

573

Declarations

References

1. C. Scheuer et al., AISI 420 martensitic stainless steel corrosion resistance enhancement by low-temperature plasma carburizing. Electrochim. Acta **317**, 70–82 (2019)
2. A. Dalmau, C. Richard, A. Igual-Muñoz, Degradation mechanisms in martensitic stainless steels: wear, corrosion and tribocorrosion appraisal. Tribol. Int. **121**, 167–179 (2018)
3. P. Dabreo et al., Estimation of tool life by industrial method and Taylors method using coated carbide insert in turning of workmaterial Ss316l. IOP Conf. Series: Mater. Sci. Eng. **1070**, 012101 (2021)
4. D. Palanisamy et al., Experimental investigation on surface integrity during machining of AISI 420 steel with tungsten carbide insert. Mater. Today Proc. **22**, 992–997 (2020)
5. N. Sharma, K. Gupta, Influence of coated and uncoated carbide tools on tool wear and surface quality during dry machining of stainless steel 304. Mater. Res. Express **6**(8), 086585 (2019)
6. M.H.S. Elmunafi, Influence of cutting condition on chip morphology when turning hardened stainless steel using coated carbide cutting tools under minimum quantity of lubrication. in AIP Conference Proceedings. 2020. AIP Publishing LLC
7. A. Panda, S. Ranjan Das, D. Dhupal, Machinability investigation of HSLA steel in hard turning with coated ceramic tool: assessment, modeling, optimization and economic aspects. J. Adv. Manuf. Syst. **18**(04), 625–655 (2019)
8. E. Basihos, F. Erzincanli, Machinibility of AISI 420 stainless steel depending on cutting speed, tool nose radius and tool coating. J. Eng. Res. Appl. Sci. **8**(1), 1127–1131 (2019)
9. M.K. Alam et al., Mechanical behavior of additive manufactured AISI 420 martensitic stainless steel. Mater. Sci. Eng. A **773**, 138815 (2020)
10. M. Kaladhar, Optimization of machining parameters when machining beyond recommended cutting speed. World J. Eng. **17**, 739–749 (2020)
11. A. Zerti et al., Prediction of machining performance using RSM and ANN models in hard turning of martensitic stainless steel AISI 420. Proc. Inst. Mech. Eng. C J. Mech. Eng. Sci. **233**(13), 4439–4462 (2019)
12. C. Moganapriya et al., Influence of coating material and cutting parameters on surface roughness and material removal rate in turning process using Taguchi method. Mater. Today Proc. **5**(2), 8532–8538 (2018)
13. C. Moganapriya et al., Effect of coating on tool inserts and cutting fluid flow rate on the machining performance of AISI 1015 steel. Mater. Test. **60**(12), 1202–1208 (2018)
14. C. Moganapriya et al., Tribomechanical behavior of TiCN/TiAlN/WC-C multilayer film on cutting tool inserts for machining. Mater. Test. **59**(7–8), 703–707 (2017)
15. C. Moganapriya et al., Influence of cutting fluid flow rate and cutting parameters on the surface roughness and flank wear of TiAlN coated tool in turning AISI 1015 steel using Taguchi method. Arch. Metall. Mater. **62**(3), 1827–1832 (2017)
16. N. Patel et al., Secondary hardness enhancement in large period TiN/TaN superlattices. Surf. Coat. Technol. **254**, 21–27 (2014)
17. C. Moganapriya et al., Technical performance of nano-layered CNC cutting tool inserts—an extensive review. Mater. Today Proc. **45**, 663–669 (2021)
18. P.D. Pantula, S.S. Miriyala, K. Mitra, KERNEL: Enabler to build smart surrogates for online optimization and knowledge discovery. Mater. Manuf. Process. **32**(10), 1162–1171 (2017)
19. P.D. Pantula, K. Mitra, Towards efficient robust optimization using data based optimal segmentation of uncertain space. Reliab. Eng. Syst. Saf. **197**, 106821 (2020)
20. P.D. Pantula, K. Mitra, A data-driven approach towards finding closer estimates of optimal solutions under uncertainty for an energy efficient steel casting process. Energy **189**, 116253 (2019)
21. T. Kostadin, S. Jakovljevic, Analysis of corrosion resistance when turning martensitic stainless steel X20Cr13 under chilled air-cooling. Adv. Prod. Eng. Manag. **12**(2), 105–114 (2017)
22. M. De Paula et al., Analysis of the performance of coated carbide cutting tools in the machining of martensitic stainless steel AISI 410 in dry and mql conditions. Mater. Res. Express **6**(1), 016512 (2018)
23. N. Jeyaprakash et al., Comparison of microstructure, mechanical and wear behaviour of laser cladded stainless steel 410 substrate using stainless steel 420 and Colmonoy 5 particles. J. Iron. Steel Res. Int. **27**(12), 1446–1455 (2020)
24. C. Vishwas et al., Effect of machining parameters on surface integrity during dry turning of AISI 410 martensitic stainless steel. IOP Conf. Series Mater. Sci. Eng. **376**, 012127 (2018)
25. M. Bertolete et al., Effects of texturing the rake surfaces of cemented tungsten carbide tools by ultrashort laser pulses in machining of martensitic stainless steel. Int. J. Adv. Manuf. Technol. **98**(9), 2653–2664 (2018)
26. Z. Zhang, T. Yu, R. Kovacevic, Erosion and corrosion resistance of laser cladded AISI 420 stainless steel reinforced with VC. Appl. Surf. Sci. **410**, 225–240 (2017)
27. C. Moganapriya et al., Dry machining performance studies on TiAlSiN coated inserts in turning of AISI 420 martensitic stainless steel and multi-criteria decision making using taguchi-DEAR approach. Silicon **2021**, 1–14 (2021)
28. C. Moganapriya et al., Achieving machining effectiveness for AISI 1015 structural steel through coated inserts and grey-fuzzy coupled Taguchi optimization approach. Struct. Multidiscip. Optim. **63**(3), 1169–1186 (2021)
29. S. Nandhakumar, R.S. Prakash, Parametric optimization in CNC turning of martensitic stainless steel 416 using Taguchi method. J. Chem. Pharm. Sci. ISSN **974**, 2115 (2017)
30. G. Cukor et al., Sustainable turning of martensitic stainless steel. Trans. FAMENA **43**(3), 1–12 (2019)
31. J.G. Corrêa, R.B. Schroeter, Á.R. Machado, Tool life and wear mechanism analysis of carbide tools used in the machining of martensitic and supermartensitic stainless steels. Tribol. Int. **105**, 102–117 (2017)
32. V. Prabakaran, Wear mechanism and tool performance of TiAlN coated during machining of AISI410 Steel. J. Bio Tribo-Corros. **4**(4), 1–9 (2018)
33. G.C. Rosa et al., Wear analysis of ultra-fine grain coated carbide tools in hard turning of AISI 420C stainless steel. Wear **376**, 172–177 (2017)
34. M. Chinnasamy et al., A frontier statistical approach towards online tool condition monitoring and optimization for dry turning operation of SAE 1015 steel. Archiv. Metall. Mater. **66**(3), 901–909 (2021)